

## EFFECT OF ECR PLASMA EXPOSURE ON THE OPTICAL PROPERTIES OF $\text{Se}_{80}\text{Te}_{20-x}\text{Pb}_x$ THIN FILMS

K. P. TIWARY\*, S. K. SINHA, SHAMSHAD A. KHAN<sup>a</sup>, L. S. S. SINGH<sup>a</sup>,  
M. HUSAIN<sup>a</sup>, Z. H. ZAIDI<sup>a</sup>

*Department of Applied Physics, Birla Institute of Technology, Patna-800014, India*

*<sup>a</sup>Department of Physics, Jamia Millia Islamia, New Delhi-110025, India*

Thin films of  $\text{Se}_{80}\text{Te}_{20-x}\text{Pb}_x$  ( $x = 2, 6$  and  $10$ ) of thickness  $3000\text{\AA}$  were prepared on a glass substrate by the vacuum evaporation technique. The optical band gap for thin films before and after exposing to ECR plasma discharge have been studied as a function of photon energy in the wavelength region  $400\text{-}900\text{ nm}$ . Thin films were exposed to plasma discharge of  $\text{CCl}_2\text{F}_2/\text{Ar}/\text{O}_2$  at a pressure ranges between  $0.015$  to  $0.020$  mbar, exposure time  $5$  minutes and rf power density  $0.39\text{ W/cm}^2$ . It was found that the optical band gap of the film increases after exposing to ECR plasma discharge. The change in optical band gap may be due to the increase in the grain size and the reduction in the disorderness of the system.

(Received November 3, 2008; accepted November 12, 2008)

*Keywords:* Thin films, Optical band gap, ECR plasma

### 1. Introduction

There has been a rapidly growing interest in the physical properties of amorphous solids during last decade. Chalcogenide glasses are practically used as optical materials in a number of cases. Therefore, their transparence characteristics have to include both the visible and close infrared part of the spectrum, practically the wavelengths of He-Ne ( $0.6328\text{ }\mu\text{m}$ ) and  $\text{CO}_2$  ( $10.6\text{ }\mu\text{m}$ ) lasers [1]. It is well known that the amorphous films are more transparent than the crystalline ones [2-3]. The optical memory effects in amorphous semiconductor films have been investigated and utilized for various applications in recent years [4-8]. These have distinct advantages, viz., large packing density, mass replication, fast data rate, high signal to noise ratio and high immunity to defects [4-9]. The use of these films for reversible optical recording by the amorphous to crystalline phase change has recently been reported by a number of workers [10-12]. The optical band gap is one of the most significant parameters in amorphous semiconducting thin films. Films are ideal specimens for reflectance and transmittance type measurements. Therefore, an accurate measurement of the optical constants is extremely important. Chalcogenide glasses have been found to exhibit the change in refractive index under the influence of light, which makes it possible to use these materials to record not only the magnitude but also the phase of illumination.

Plasma plays a significant role in thin film processes namely, deposition and etching by sputtering and by plasma assisted chemistry, resulting in many ways of developing sophisticated technological plasma process [13]. In the present work, we have chosen Se because of its wide commercial applications. Its device applications like switching, memory and xerography etc. made it attractive. It also exhibits a unique property of reversible transformation [14]. This property makes very useful in optical memory devices. But in pure state, it has disadvantages because of its short lifetime and low sensitivity. To overcome these difficulties certain additives are used [15-

---

\*Corresponding author: kptiwary@rediffmail.com

19], especially the use of Se-Te, Se-Sb and Se-In alloy is of interest owing to their various properties like greater hardness, higher sensitivity, higher crystallization temperature, higher conductivity and smaller aging effects as compared to pure amorphous Se [20]. Here we have chosen Te as an additive to overcome these problems. In the present work, we have incorporated Pb in the Se-Te system. The addition of third element will create compositional and configurational disorder in the material with respect to the binary alloy. The present work deals with a comparative study of the optical constants of the amorphous films and the optical constants of the thin films when exposed to ECR plasma.

## 2. Experimental Procedure

Glassy alloys of  $\text{Se}_{80}\text{Te}_{20-x}\text{Pb}_x$  with  $x=2,6$  and  $10$  were prepared by quenching technique. The highly pure materials were weighed using electronic balance according to their atomic percentages and sealed in quartz ampoules in a vacuum of  $10^{-5}$  Torr. The sealed ampoules were then placed in a Microprocessor-controlled Programmable Muffle Furnace at  $1123$  K for  $12$  hours. The ampoules were rocked frequently to ensure the homogenization of the melt. After that the quenching was done in ice water to obtain the amorphous state. Thin films of glass alloys of thickness  $3000\text{\AA}$  were prepared by the vacuum evaporation technique in which the glass substrate was kept at room temperature ( $300\text{K}$ ) at a base pressure of  $10^{-6}$  Torr using a molybdenum boat. The films were kept inside the deposition chamber for  $24$  hours to achieve the metastable equilibrium as suggested by Abkowitz [21]. The thickness of the films was measured using a single crystal thickness monitor.

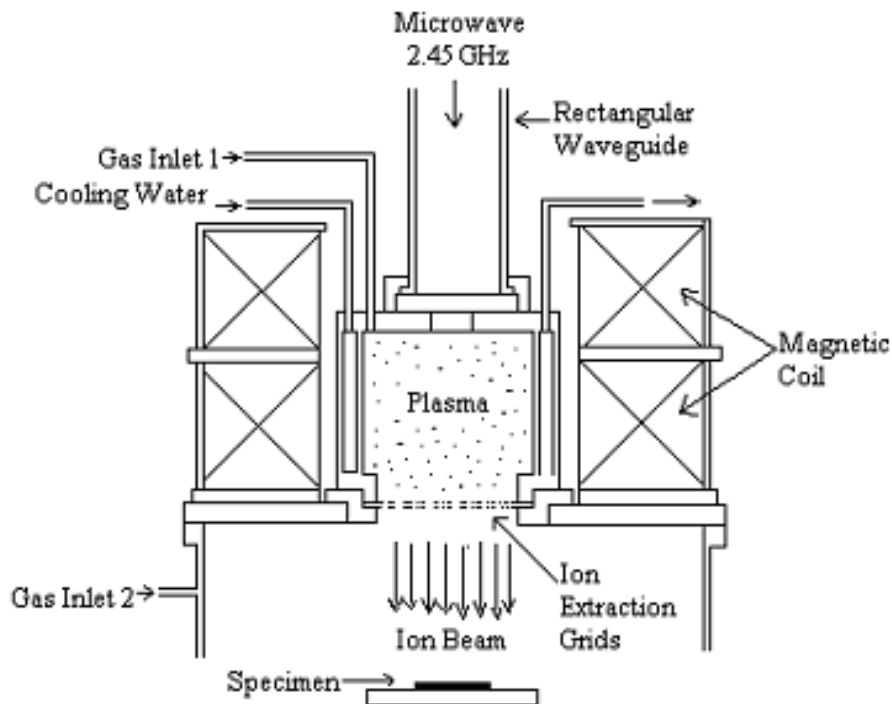


Fig.1. ECR Plasma system.

The samples were then exposed to  $\text{CCl}_2\text{F}_2/\text{Ar}/\text{O}_2$  discharge inside the ECR plasma chamber. ECR plasma source is RR 160 PQ. In this source there is a plasma chamber where the plasma is produced due to the ionization and excitation of the neutral particles. The microwave is generated by a magnetron through a power supplier SM 445 that generates power up to  $1250$  W and transmitted by a waveguide system. At a frequency of microwaves of  $2.46$  GHz and  $875$  Gauss of magnetic field, plasma are generated inside the plasma chamber when the electrical field

lines of the microwaves (axial component) and magnetic field lines of the magnetic field (radial component) stand perpendicular to each other and gyration frequency of the electrons in the magnetic field is equal to microwave frequency. In this experiment plasma exposure time for all the samples were kept 5 minutes and rf power density was  $0.39 \text{ W/cm}^2$ . A vacuum system is necessary for generation of a base pressure of  $\geq 10^{-6}$  mbar which enables a gas flow through the ECR plasma source of  $\geq 50$  sccm/min in the pressure range of  $(1-5) \times 10^{-3}$  mbar. A sufficient gas flow is required for this operation in which the vacuum level is not disturbed. ECR plasma system is shown schematically in fig.1. After exposing the amorphous thin films to ECR plasma, optical band gap were measured. A JASCO, V-500, UV/VIS/NIR spectrophotometer was used for measuring optical absorption. The optical absorption and reflectance were measured for as deposited thin films and after exposing to ECR plasma on  $\text{Se}_{80}\text{Te}_{20-x}\text{Pb}_x$  thin films as a function of wavelength (400-900 nm) and incident photon energy.

### 3. Result and discussion

The variation of the absorption coefficient ( $\alpha$ ) as a function of incident photon energy ( $h\nu$ ) for deposited thin films and after exposing to ECR discharge of a  $\text{Se}_{80}\text{Te}_{20-x}\text{Pb}_x$  are shown in fig.2 and fig.3 respectively. The absorption coefficient ( $\alpha$ ) has been obtained directly from the absorbance against wavelength curves using the relation [22-30]

$$\alpha = \text{OD}/t \quad (1)$$

where OD is the optical density measured at a given layer thickness(t).

It has been observed that the value of absorption coefficient ( $\alpha$ ) increases linearly with the increase in photon energy for as deposited and after exposing to ECR discharge on a  $\text{Se}_{80}\text{Te}_{20-x}\text{Pb}_x$  thin films. The values of absorption coefficient ( $\alpha$ ) for amorphous and ECR plasma exposed films at different concentrations of lead is given in Table-1. It is clear from this table that the value of absorption coefficient ( $\alpha$ ) of the films increases after exposing to ECR plasma discharge.

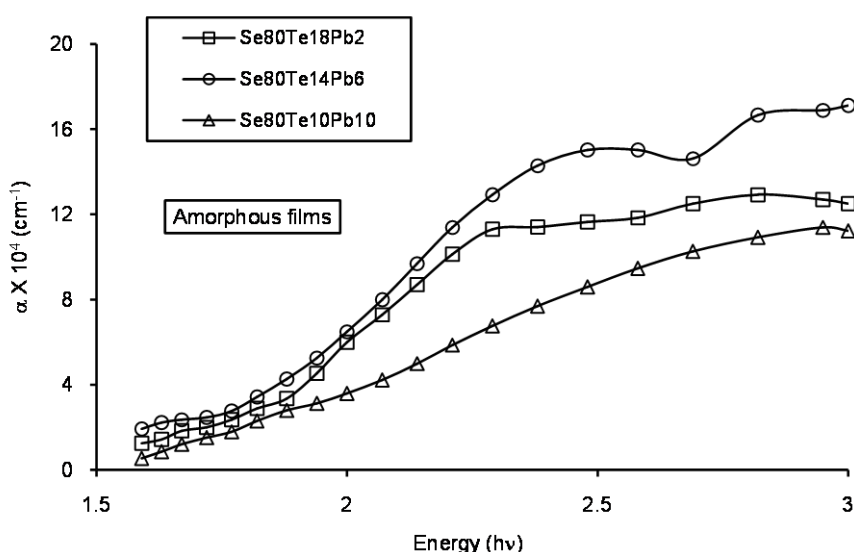


Fig.2. Absorption coefficient ( $\alpha$ ) against photon energy in amorphous  $\text{Se}_{80}\text{Te}_{20-x}\text{Pb}_x$  thin films.

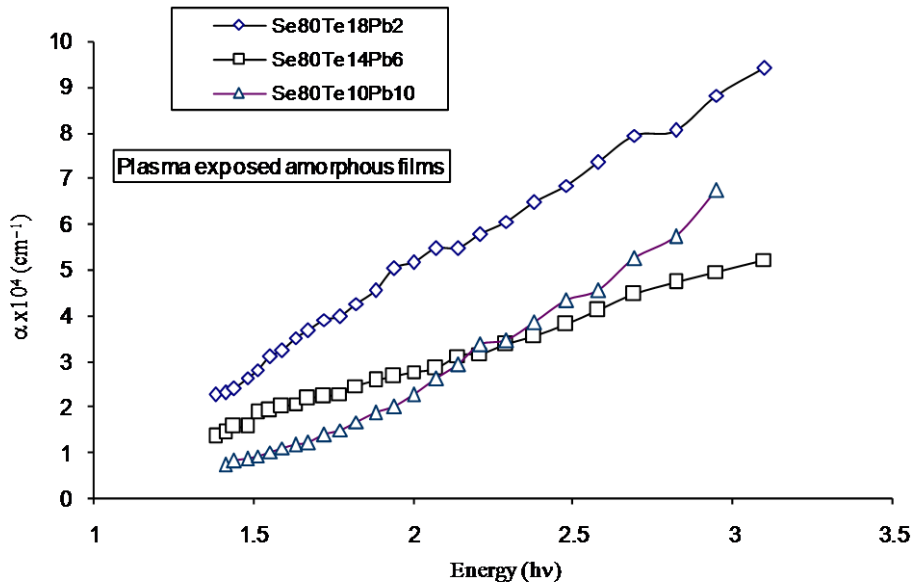


Fig.3. Absorption coefficient ( $\alpha$ ) against photon energy of ECR plasma exposed  $Se_{80}Te_{20-x}Pb_x$  thin films.

In the absorption process, a photon of known energy excites an electron from a lower to a higher energy state, corresponding to an absorption edge. In chalcogenide glasses, a typical absorption edge can be broadly ascribed to one of the three processes, firstly residual below gap absorption; secondly Urbach tails and thirdly interband absorption. Chalcogenide glasses have been found to exhibit highly reproducible optical edges, which are relatively insensitive to preparation conditions and only the observable absorption with a gap under equilibrium conditions account for the first process. In the second process the absorption edge depends exponentially on the photon energy according to the Urbach relation [31]. In the amorphous materials,  $\alpha$  increases exponentially with the photon energy near the energy gap. The optical absorption edge is given by the equation

$$\alpha \sim \exp [A(h\nu - h\nu_0)]/kT \quad (2)$$

where  $A$  is a constant of the order of unity and  $\nu_0$  is the constant corresponding to the lowest excitonic frequency. In various absorption processes, the electrons and the holes absorb both a photon and phonon. The photon supplies the needed energy, while the phonon supplies the required momentum. The variation of  $\alpha$  with photon energy can be explained in terms of fundamental absorption, exciton absorption and valence band acceptor absorption. The measurement of transmission allows us to determine the absorption coefficient i.e. the number of absorbed photons per incident photons. The present system obeys the role of indirect transition ( $m > 1$ ) and the relation between the optical band gap, optical absorption coefficient  $\alpha$  and the energy  $h\nu$  of the incident photon is given by the equation

$$(\alpha h\nu)^{1/2} \propto (h\nu - E_g) \quad (3)$$

The value of indirect optical bandgap ( $E_g$ ) has been calculated from the plot of  $(\alpha h\nu)^{1/2}$  versus photon energy ( $h\nu$ ) by taking the intercept of X-axis.

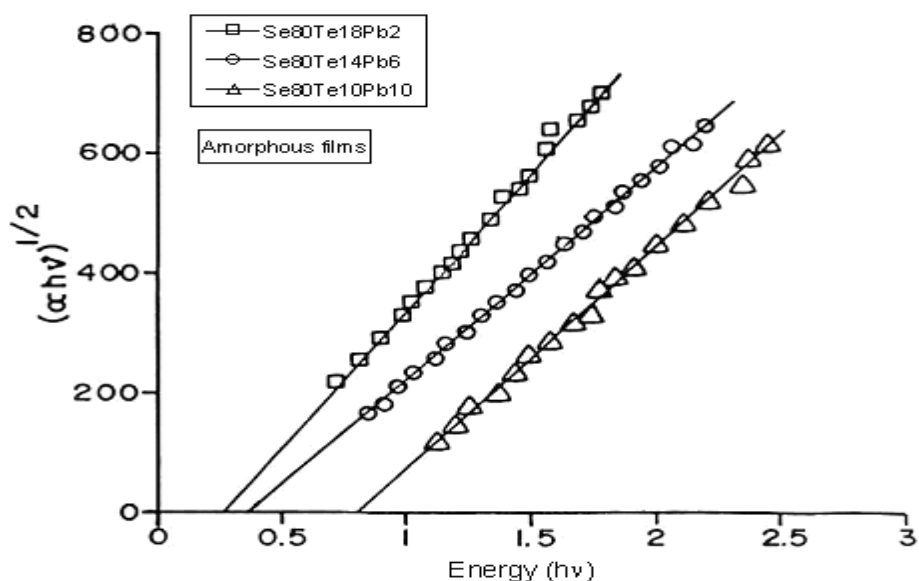


Fig.4. Variation of  $(\alpha hv)^{1/2}$  against photon energy  $(hv)$  in amorphous  $Se_{80}Te_{20-x}Pb_x$  thin films.

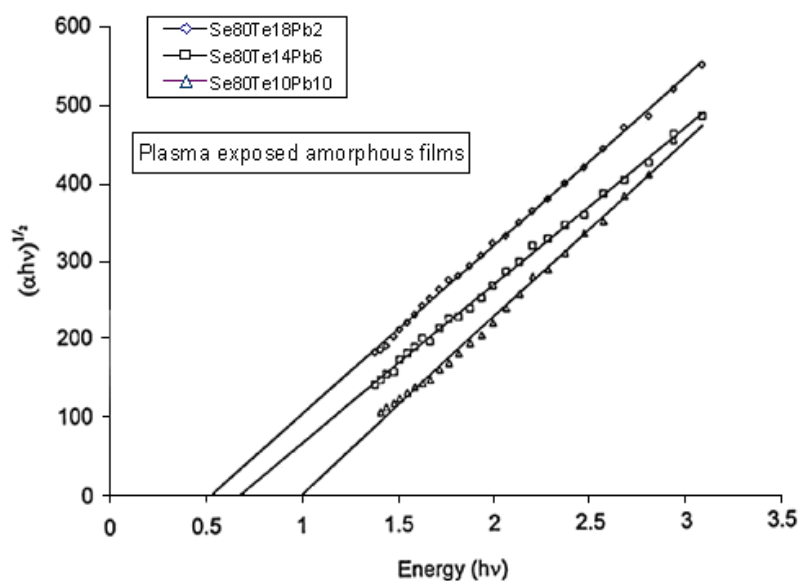


Fig. 5. Variation of  $(\alpha hv)^{1/2}$  against photon energy  $(hv)$  of ECR plasma exposed  $Se_{80}Te_{20-x}Pb_x$  thin films.

The variation of  $(\alpha hv)^{1/2}$  with photon energy  $(hv)$  for amorphous films and plasma exposed thin film of  $Se_{80}Te_{20-x}Pb_x$  are shown in fig.4 and fig.5. The value of indirect optical band gap ( $E_g$ ) has been calculated by the intercept of X-axis. The calculated values of  $E_g$  for these two cases of  $Se_{80}Te_{20-x}Pb_x$  are given in Table-2. The variation of optical band gap with Pb concentration in  $Se_{80}Te_{20-x}Pb_x$  system for two cases is shown if fig.8.

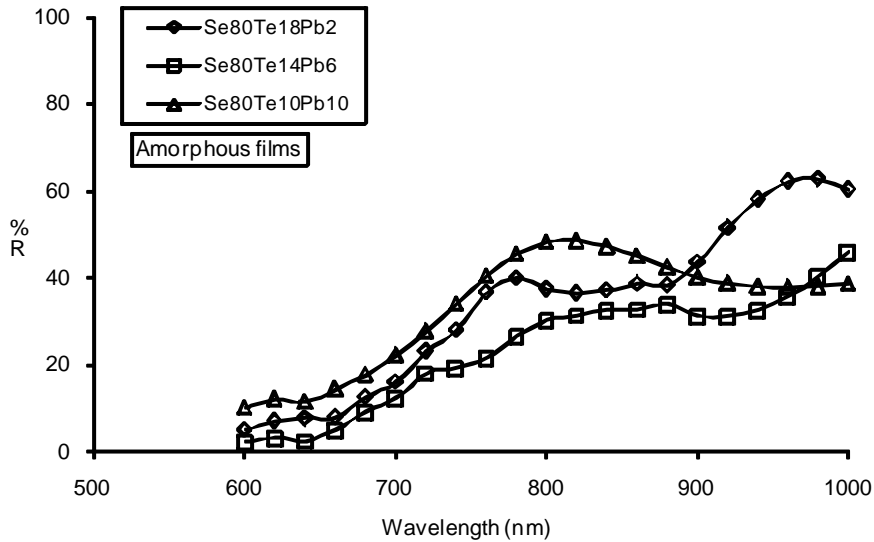
Table1. Absorption coefficient and reflectance of amorphous films and plasma exposed thin films.

Samples	Absorption coefficient( $\alpha$ ) and reflectance(R%)			
	Amorphous films		Plasma exposed films	
	$\alpha$ ( $\text{cm}^{-1}$ )	R%	$\alpha$ ( $\text{cm}^{-1}$ )	R%
$\text{Se}_{80}\text{Te}_{18}\text{Pb}_2$	$2.01 \times 10^4$	22.25	$3.9 \times 10^4$	27.25
$\text{Se}_{80}\text{Te}_{14}\text{Pb}_6$	$2.47 \times 10^4$	18.17	$2.58 \times 10^4$	29.06
$\text{Se}_{80}\text{Te}_{10}\text{Pb}_{10}$	$1.52 \times 10^4$	27.67	$1.78 \times 10^4$	34.62

Table2. Optical bandgap of amorphous films and plasma exposed thin films.

Samples	Optical Bandgap $E_g$ (eV)	
	Amorphous films	Plasma exposed films
$\text{Se}_{80}\text{Te}_{18}\text{Pb}_2$	0.27	0.51
$\text{Se}_{80}\text{Te}_{14}\text{Pb}_6$	0.38	0.62
$\text{Se}_{80}\text{Te}_{10}\text{Pb}_{10}$	0.81	1.00

Fig. 6 and Fig. 7 depict the variation of reflectance (R) for amorphous and ECR plasma exposed films with the wavelength. These figures show that the value of reflectance in both cases increases with wavelength. The values of reflectance for amorphous and after exposing ECR plasma discharge with different compositions of lead is shown in Table-1. It is clear from this table that the value of reflectance increases after exposing ECR plasma discharge.

Fig.6. Variation of reflectance (R) with wavelength in amorphous  $\text{Se}_{80}\text{Te}_{20-x}\text{Pb}_x$  thin films.

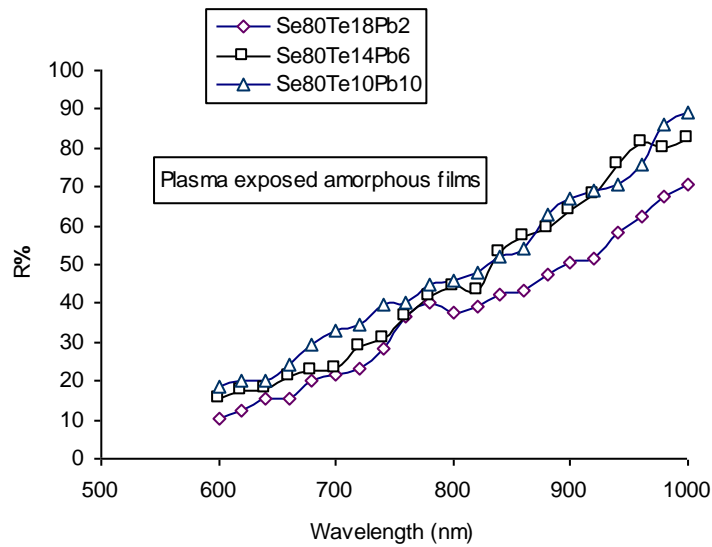


Fig.7. Variation of reflectance ( $R$ ) with wavelength of ECR plasma exposed  $Se_{80}Te_{20-x}Pb_x$  thin films.

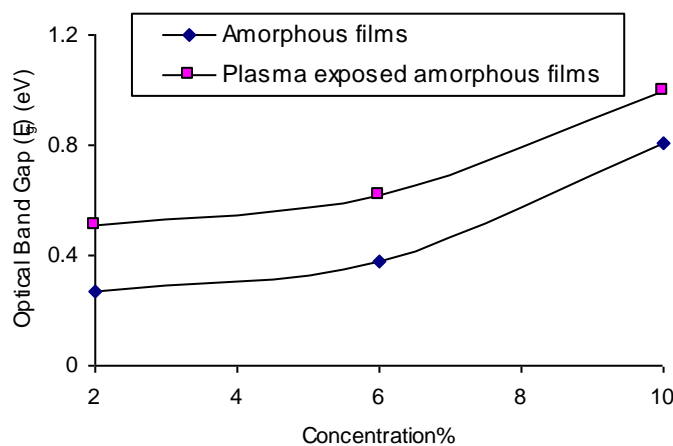


Fig.8. Variation of optical band gap ( $E_g$ ) with Pb concentration in  $Se_{80}Te_{20-x}Pb_x$  for amorphous and ECR plasma exposed films.

It is evident from Table-2 that the value of optical band gap ( $E_g$ ) increases with increasing Pb concentration. The increase in the optical band gap with increasing Pb concentration may be due to the increase in grain size, the reduction in the disorder and decrease in density of defect states (which results in the reduction of tailing of bands) [31-33]. The increase in the optical band gap could also be discussed on the basis of density of state model proposed by Mott and Davis [34]. Chalcogenide thin films always contain a high concentration of unsaturated bonds or defects. These defects are responsible for the presence of localized states in the amorphous band gap. The effect of ECR Plasma on the thin film is interpreted on the basis of amorphous crystalline transformation. After plasma exposure on amorphous films the optical band gap increases, which shows that the amorphous films became crystallized. The optical band gap increases during crystallization. After exposing to the plasma discharge, the optical band gap of the thin films  $Se_{80}Te_{20-x}Pb_x$  increases. During ECR plasma discharge, the unsaturated defects are gradually comes out and producing a large number of saturated bonds. The reduction in the number of unsaturated defects decreases the density of localized states in the band structure consequently increasing the optical band gap.

#### 4. Conclusion

The optical absorption measurements on the  $\text{Se}_{80}\text{Te}_{20-x}\text{Pb}_x$  thin films after exposing ECR plasma discharge indicate that the absorption mechanism is due to indirect transition. The effect of ECR plasma exposure is interpreted on the basis of change in optical band gap. The optical band gap increases after exposing to ECR plasma discharge and also Pb concentration. This may be due to the decrease in the density of defect states, which results in a reduction in the tailing of the bands. Due to large absorption coefficient and compositional dependence of reflection, these materials may be suitable for optical data storage.

#### References

- [1] D. M. Petrovic, S. R. Lukic, M. J. Avramov, V. V. Khimintes, *J. Mater. Sci. Lett.* **5**, 290 (1986).
- [2] L. Zdanowicz, B. Jarzabek, *J. Non-cryst. Solids* **97/98**, 1203 (1987).
- [3] L. Bdanovic, T. Kwiecien, *Vacuum* **27**, 409 (1977).
- [4] J. Feinleib, J. DeNeufville, S. C. Mose, S. R. Ovshinsky, *Appl. Phys. Lett.* **18**, 254 (1971).
- [5] K. A. Rubin, M. Chen, *Thin Solid Films* **181**, 129 (1989).
- [6] S. Y. Suh, D. A. Snyder, D. L. Anderson, *Appl. Opt.* **24**, 868 (1985).
- [7] P. F. Carcia, F. D. Kalk, P. E. Beirstedt, A. Ferretti, G. A. Jones, D. G. Swariz, *J. Appl. Phys.* **64**, 1715 (1988).
- [8] S. Zembutsu, Y. Toyoshima, T. Igo, H. Nagai, *Appl. Opt.* **14**, 3073 (1975).
- [9] Y. Maeda, H. Andoh, I. Ikuta, H. Minemura, *Appl. Opt.* **64**, 1715 (1988).
- [10] D. P. Gosain, T. Shimizu, M. Ohmura, M. Suzuki, T. Bando, S. Okano, *J. Mater. Sci.* **26**, 3271 (1991).
- [11] Shamshad A. Khan, M. Zulfequar, M. Husain, *Vacuum* **72**, 291 (2004).
- [12] D. J. Gravesteiju, *Appl. Opt.* **27**, 736 (1988).
- [13] Morito Matsuoka, Ken'ichi Ono, *J. Vac. Sci. Technol., A* **6** (1), 25 (1988).
- [14] K. Tanka, *Phys. Rev. B* **39**, 1270 (1989).
- [15] M. M. Hafiz, A. M. Moharram, M. A. Abdel-Rahim, *Thin Solid Films* **292**, 7 (1997).
- [16] Y. Murakami, A. Sawata, Y. Tsuru, *J. Mater. Sci.* **34**, 951 (1999).
- [17] Jee Yeob Shim, Sang Wook Park, Hong Koo Baik, *Thin Solid Films* **292**, 31 (1997).
- [18] J. M. Saitar, J. Ledru, A. Hamou, G. Saffarini, *Physica B* **245**, 256 (1998).
- [19] J. Vazquez, C. Wagmer, P. Villares, *J. Non-Cryst. Solids* **235**, 548 (1998).
- [20] S. K. Srivastava, A. Kumar, *Physica B*, **183**, 409 (1993).
- [21] M. Abkowitz, G. M. T. Foley, A. C. Palumbo, *AIP Conf. Proc.* **120**, 117 (1984).
- [22] K. Oe, Y. Toyoshiman, H. Nagai, *J. Non-Cryst. Solids* **20**, 405 (1976).
- [23] H. Keller, J. Stuke, *Phys. Stat. Sol.* **8**, 831 (1965).
- [24] T. Igo, Y. Toyoshima, *J. Non-Cryst. Solids* **58**, 304 (1973).
- [25] S. Chaudhari, S. K. Biswas, A. Choudhary, *J. Non-Cryst. Solids* **23**, 4470 (1998).
- [26] N. Sharoff, A. K. Chakravarti, *Opt. Mem: Tech and Application*, September (1991).
- [27] E. K. Shokr, M. M. Wakkad, *J. Non-Cryst. Solids* **23**, 1197 (1992).
- [28] J. Tauc In., J. Tauc ed, *Amorphous and Liquid Semiconductors* New York: Plenum Press **159**, (1979).
- [29] A. K. Agnihotri, A. Kumar, A. N. Nigam, *Philos. Mag B* **57**, 319 (1988).
- [30] A. Kumar, M. Husain, S. Swarup, A. N. Nigam, *Physica B* **162**, 177 (1990).
- [31] F. Urbach, *Phys. Rev.* **92**, 1324 (1953).
- [32] M. Ilyas, M. Zulfequar, M. Husain, *J. Modern Optics* **47**, 663 (2000).
- [33] T. T. Nang, M. Okuda, T. Matsushita, S. Yokota, A. Suzuki, *Jap. J. App. Phys.* **14**, 849 (1976).
- [34] N. F. Mott, E. A. Davis, *Electronic Processes in Non-Cryst. Mater.* (Oxford: Clarendon) 428, (1979).